Autonomic Neuroscience: Basic and Clinical 218 (2019) 16–24

Contents lists available at ScienceDirect

Autonomic Neuroscience: Basic and Clinical

journal homepage: www.elsevier.com/locate/autneu

Thoracic sympathetic chain stimulation modulates and entrains the respiratory pattern

R.R. Dhingra[a], G. Kola[b], S.J. Lewis[b], M. Dutschmann[a,*]

[a] Division of Systems Neurophysiology, The Florey Institute of Neuroscience & Mental Health, Melbourne, Australia
[b] Division of Pediatrics, Department of Medicine, Case Western Reserve University, Cleveland, OH, USA

ARTICLE INFO

Keywords:
Sympathetic chain
Intra-abdominal pressure
Hering-Breuer reflex
Entrainment
Visceral spinal afferent
Locomotor-respiratory coupling

ABSTRACT

Stimulation of thoracic sympathetic chain (TSC) afferents has been shown to slow the respiratory rhythm in dogs, monkeys and humans. However, sparse information exists about the physiological role of TSC afferents in modulating respiration or the central pathways of these afferents. Here, we sought to investigate whether the perfused preparation of juvenile rats is a suitable experimental model to study the role of TSC-afferents in the modulation of respiration. We show that tonic (30s) TSC stimulation initially triggered either prolonged post-inspiratory vagal nerve discharge, or when the stimulus onset occurred in the second half of expiration, TSC stimulation also modulated late-expiratory abdominal nerve activity. Independent of the timing of the TSC-stimulation the net effect was lengthening of the expiratory interval and subtle shortening of inspiration. TSC evoked respiratory modulation showed progressive habituation during the stimulus period. Importantly, high thoracic spinal cord transections abolished the TSC-evoked respiratory modulation, indicating that TSC afferents are likely to be relayed within the thoracic spinal cord. Next, we repeatedly applied 400 ms trains of stimuli at an inter-burst interval near that of the intrinsic respiratory rate and show that rhythmic TSC stimulation has a strong potential to entrain the central respiratory rhythm. Importantly, under the imposed rhythm, TSC stimuli became aligned with the late expiratory phase. The entrainment pattern supports the hypothesis that the TSC pathway may convey extra-pulmonary visceral mechano-sensory feedback that might be sensitive to visceral mass movements during locomotion. The latter was previously discussed to significantly contribute to the locomotor–respiratory coupling in various mammalian species.

1. Introduction

The respiratory rhythm is generated by a ponto-medullary central pattern generator network (Ausborn et al., 2018; Del Negro et al., 2018; Dutschmann and Dick, 2012; Lindsey et al., 2012; Ramirez and Baertsch, 2018; Smith et al., 2009). However, the centrally generated respiratory rhythm and pattern can be modulated by peripheral sensory inputs to adapt breathing to behavior and metabolic demands. Autonomic sensory inputs can be broadly classified into two classes: regulatory inputs, which modulate rate and/or amplitude of the breathing pattern, and transformative inputs, which evoke distinct respiratory or non-respiratory behaviors such as sniffing (Pérez de los Cobos Pallares et al., 2016), swallowing (Bautista and Dutschmann, 2014; Jean, 2001) or coughing (Bolser et al., 2015; Mutolo, 2017). The most well studied regulatory respiratory reflexes are the respiratory chemoreflex of the carotid bodies and the vagal Hering-Breuer reflex. Carotid body chemoreceptors are tonically active and modulate the drive to breathe (Biscoe and Taylor, 1963; Eyzaguirre and Lewin, 1961; Prabhakar and Peng, 2004; Taylor, 1968), whereas the Hering-Breuer reflex (HBR) acts phasically on inspiratory on- and off-switch mechanisms (Clark and von Euler, 1972; Cohen et al., 1993; Kubin et al., 2006; von Euler, 1980; Zuperku et al., 1982).

In the present study, we are concerned with the breadth of autonomic sensory afferent modalities that can modulate the respiratory motor pattern. For instance, Romaniuk et al. (1993) identified a thoracic mechanosensory reflex that persisted after bilateral vagotomy in dogs, and interpreted their findings to reflect the influence of intercostal muscle spindle afferents on respiration. Similarly, Kruta et al. (1950) first demonstrated that stimulation of splanchnic sympathetic afferents, also called visceral spinal afferents, could produce apnea in humans. Later investigation by Kostreva et al. (1978) confirmed that stimulation of lower thoracic sympathetic chain afferents (and any

* Corresponding author at: Division of Systems Neurophysiology, The Florey Institute of Neuroscience & Mental Health, 30 Royal Parade, Parkville, VIC 3052, Australia.
E-mail address: mathias.dutschmann@florey.edu.au (M. Dutschmann).

https://doi.org/10.1016/j.autneu.2019.01.008
Received 22 November 2018; Received in revised form 29 January 2019; Accepted 30 January 2019
1566-0702/ © 2019 Published by Elsevier B.V.

sympathetic ganglion from T1 to T12) could inhibit respiration in dogs and monkeys. In vivo, lower thoracic visceral spinal afferents arising from abdominal viscera and coursing through sympathetic nerves are thought to mediate both homeostatic and nociceptive reflexes (for review, see Cervero, 1994; Cervero and Jänig, 1992; Jänig, 1996). However, little information exists regarding the organization and physiological role of these visceral spinal afferent pathways (Cervero, 1985; Ossipov et al., 2010).

Thus, the first goal of the present study was to assess whether stimulation of sympathetic visceral spinal afferents modulates the respiratory pattern in rodents. If so, the in situ perfused brainstem preparation of rat could provide a valuable tool to identify and investigate the organization of the brainstem circuits that process visceral spinal inputs.

In the present study, by stimulating thoracic sympathetic chain (TSC) afferents in situ, we confirm the existence of sympathetic afferent pathways that mediate a slowing of the respiratory pattern via projections into the thoracic spinal cord in rats. To further investigate the physiological role of TSC-evoked modulation of breathing we investigated the effect of rhythmic TSC stimulation on the respiratory rhythm. If we consider that the respiratory network generates the slow oscillation of breathing which is coupled to its sensory inputs, examination of the synchronization of the network by the inputs can offer insight into the sensory-motor integration of the respiratory network (Dhingra et al., 2017, 2013; Oku et al., 1993; Oku and Dick, 1992; Zhu et al., 2013). Our data indicate that TSC-afferents have the capacity to entrain breathing and thereby may convey regulatory sensory feedback for the respiratory central pattern generator. Thus, we speculate that in vivo, TSC afferents may provide rhythmic sensory feedback arising from extra-pulmonary visceral mechanoreceptors that might be sensitive to visceral mass movements, for example, during locomotion.

2. Material and methods

Experimental protocols were approved by and conducted with strict adherence to the guidelines established by the Animal Ethics Committee of The Florey Institute of Neuroscience & Mental Health, Melbourne, Australia.

2.1. Perfused brainstem-spinal cord preparation

Experiments were performed in juvenile Sprague-Dawley rats of either sex (N = 48 rats, 17–30 days post-natal) using the arterially perfused in situ brainstem-spinal cord preparation as described previously (Dhingra et al., 2017; Dutschmann et al., 2000; Paton, 1996). Briefly, rats were anesthetized by inhalation of isoflurane (2%) until they reached a surgical plane of anesthesia. The rats were then transected below the diaphragm and transferred to an ice-cold bath of artificial cerebrospinal fluid (aCSF, in mM: 125 NaCl, 3 KCl, 1.25 KH_2PO_4, 2.5 $CaCl_2$, 1.25 $MgSO_4$, 25 $NaHCO_3$, 10 D-glucose) for pre-collicular decerebration. After decerebration, the lungs and heart were removed. Next, the descending aorta, left phrenic, and left vagal nerves were prepared for later cannulation and recording. The preparation was then transferred into a recording chamber. The descending aorta was cannulated with a double-lumen catheter for perfusion and measurement of perfusion pressure. The preparation was perfused with aCSF containing sucrose (4.5×10^{-3} g/mL) for oncotic pressure, warmed to 31 °C using a peristaltic pump, recirculating water bath and heat exchanger (ELMI, TW-2.02). The perfusion circuit also contained two bubble traps and a nylon filter (Millipore, 100 μm pore size) to prevent embolism. The perfusate was continually bubbled with carbogen (95% O2/5% CO2) to maintain constant chemosensory drive. Phrenic, vagal, hypoglossal and iliohypogastric nerves were mounted in suction electrodes to measure respiratory motor output. Nerve potentials were amplified (10,000×, Warner Instruments, DP-311), filtered (0.01–10 kHz), digitized (AD Instruments, PowerLab 16/35) and stored on a computer using LabChart software (AD Instruments). Upon resumption of apneustic respiratory motor output, the preparation was tuned to produce a eupnea-like output by administering a bolus of NaCN (0.1–0.3 mL, 0.1% w/v). The TSC (T7–T10) was then dissected for later stimulation.

2.2. Experimental protocol

After recording at least 10 min of eupnea-like baseline activity, we stimulated the TSC via a bipolar suction electrode coupled to a stimulus isolation unit (A.M.P.I., ISO-flex) and stimulus generator (A.M.P.I., Master-8). The spinal root of the sympathetic ganglion rostral to the stimulation site was cut to allow the stimulation electrode and cut end of the sympathetic chain to be suspended in air. Stimuli consisted of 30s trains with a pulse frequency of 10 Hz and pulse duration of 100 μs. Several stimulation trials were acquired with different current amplitudes to determine the activation threshold. Trials were separated by at least 1 min to avoid evoking any rapid sensitization or habituation of the TSC afferent pathway.

In a subset of experiments, following measurement of the baseline response to TSC stimulation, we transected the thoracic spinal cord (T1) to determine whether TSC afferents mediated their effects via a spinal cord relay. After acquisition of baseline TSC stimulation responses, we dissected the descending aorta from the thoracic wall and then transected the thoracic spinal cord and sympathetic chain. In subsequent experiments, we pithed the thoracic spinal cord with a hypodermic needle to avoid any disruption of the thoracic sympathetic chain in case TSC afferent fibers projected rostrally through the sympathetic chain. Because both perturbations yielded qualitatively similar results, we grouped data from both protocols to assess whether TSC afferents project into the spinal cord.

Finally, in another subset of experiments, we assessed the ability of TSC afferents to entrain the respiratory rhythm. To do so, we first measured the intrinsic frequency of each preparation immediately before the entrainment trial. Then, we stimulated the TSC rhythmically with an inter-burst interval that matched the intrinsic frequency of respiration (burst duration: 0.4 s, pulse frequency: 20 Hz, pulse width 100 μs). The current amplitude for entrainment trials was always at least 1.5× the threshold current necessary to evoke a slowing of the respiratory pattern. TSC forcing trials lasted for at least 300 s to ensure that we recorded sufficient cycles to accurately determine the significance of the entrainment interaction (see Section 2.3 Data analysis & Figs. 5–8).

2.3. Data analysis

To determine respiratory phase durations, PNA was first high-pass filtered (300 Hz), rectified and integrated with a low-pass filter (1 Hz). All filtering was performed in forward-backward mode to prevent phase distortion. A threshold crossing algorithm was used to determine the onset and offset times of the integrated PNA time series. Events were manually inspected to identify and remove any artifacts. From these event times, we measured the mean respiratory period (T_{TOT}), inspiratory (T_I) and expiratory (T_E) durations at baseline, during and after TSC stimulation. Note that all respiratory cycles recorded at baseline, during or after TSC stimulation were used to determine mean respiratory phase durations.

The activation threshold for the respiratory modulation evoked by TSC stimulation was determined by fitting the relationship between TSC stimulus current strength and the fold change in the respiratory period with a logistic function.

To assess the mean effect of a continuous 30s train of TSC stimulation on the respiratory pattern, we considered only responses from trials using a stimulus current of 1.5× the threshold to evoke an HBR-like response. All supra-threshold responses were considered as replicates and averaged before evaluating the statistical significance of

changes in respiratory phase durations evoked by TSC stimulation.

The analytic methods used to assess the entrainment of the respiratory rhythm by rhythmic TSC stimulation were described in previous publications (Dhingra et al., 2017, 2013; Zhu et al., 2013). Briefly, entrainment by TSC stimulation was evaluated using PNA as an index of the fictive breathing pattern. We used the Hilbert transformation to extract the instantaneous phases of PNA and the TSC stimulus. To do so, protophases of PNA and the TSC stimulus were determined via the Hilbert transform of the band-pass filtered, integrated signals. Protophases were corrected to obtain true instantaneous phases using the transformation defined in Kralemann et al. (2008). While the onset of PNA is not associated with an instantaneous phase of 0 in this convention, the instantaneous relative phase, $\phi_{PNA} - \phi_{TSC}$, is convenient to qualitatively identify the existence of entrainment because entrainment is indicated by periods where the instantaneous relative phase is approximately constant. Note that the absolute values of the instantaneous relative phase during synchronized regions of the time series indicate the relative phase lag between PNA and the TSC stimulus.

To quantitatively assess whether a significant entrainment interaction existed in a given trial, we compared the mutual information of the instantaneous phases with that of a bootstrap distribution. Mutual information quantifies the dependence (linear or nonlinear) between two variables. Thus, the mutual information of the instantaneous phase of PNA and the instantaneous phase of the TSC stimulus quantifies the strength of the entrainment of PNA by the TSC forcing. We used a fixed number of bins (100) to discretize the joint-probability distribution. To assess the statistical significance of the entrainment interaction in a given TSC forcing trial, we used a bootstrap surrogate data testing approach. The bootstrap distribution was generated by shuffling whole cycles of both instantaneous phase time series before computing the mutual information of the instantaneous phases. For each TSC forcing trial, a bootstrap distribution that consisted of 100 shuffled surrogates was generated. If the mutual information of original instantaneous phase time series' was greater than the upper bound of the 99th percentile of the bootstrap distribution, then the entrainment interaction between PNA and the TSC stimulus was considered significant.

All analyses were performed using custom routines implemented in MATLAB. Statistical comparisons were made after averaging replicates using a one-way repeated measures ANOVA followed by Tukey's Honestly Significant Differences (HSD) post-hoc test. Unless stated otherwise, all data are presented as mean ± standard deviation.

3. Results

3.1. Stimulation of the thoracic sympathetic chain evokes a slowing of the respiratory rhythm

A representative response to TSC stimulation is shown in Fig. 1. TSC stimulation evoked a slowing of the respiratory rhythm. The TSC-evoked respiratory slowing rapidly habituated within the 30s stimulus duration such that the respiratory period of the later cycles approached that of the baseline period. After the stimulus, the frequency of the respiratory rhythm transiently increased above baseline levels. Interestingly, we noted a phase-dependence of TSC stimulation on the evoked respiratory motor pattern. When the stimulus began during late expiration, as shown in Fig. 1A, TSC stimulation initially prolonged the discharge of late-expiratory ANA. However, in subsequent cycles, persistent post-inspiratory discharge of VNA prolonged the respiratory period, whereas ANA remained similar to baseline. When the TSC stimulus began during inspiratory or post-inspiratory phases, as shown in Fig. 1B, the TSC-modulated respiratory motor pattern consisted solely of enhanced post-inspiratory VNA.

The effects of TSC stimulation on the respiratory pattern are quantified for the group in Fig. 2. TSC stimulation significantly increased the respiratory period (T_{TOT} at baseline, 4.41 ± 1.93 s, versus during TSC stimulation, 5.53 ± 2.28 s, $p < 0.05$, N = 13 experiments). After stimulation, the respiratory period tended to decrease below baseline levels. TSC stimulation modestly, but significantly reduced the duration of inspiration (T_I at baseline, 0.84 ± 0.22 s, versus during TSC stimulation, 0.80 ± 0.20 s, $p < 0.01$, N = 13 experiments). Inspiratory phase duration quickly returned to baseline levels after the stimulus. Finally, TSC stimulation significantly increased the duration of the expiratory phase (T_E at baseline, 3.57 ± 1.75 s, versus during TSC stimulation, 4.73 ± 2.12 s, $p < 0.05$, N = 13 experiments). The T_E prolongation appeared largely related to pronged post-inspiratory discharge in VNA (see Fig. 1). Taken together, TSC stimulation modulates the respiratory pattern through a modulation of expiratory activity.

Next, we determined the threshold for respiratory rhythm modulation by TSC stimulation by fitting the change in the respiratory period evoked during all TSC stimulation trials with a logistic function (Fig. 3). The threshold to prolong the respiratory period by TSC stimulation was 98.7 μA ($R^2 = 0.117$, $p = 2.7 \times 10^{-8}$, n = 93 trials, N = 24 experiments).

3.2. Thoracic sympathetic chain afferents modulate the respiratory pattern via a spinal-cord pathway

We next tested whether TSC afferents project via the spinal cord by measuring the response to TSC stimulation before and after either thoracic spinal cord transection or pithing the thoracic spinal cord (which maintained the integrity of the thoracic sympathetic chain). Representative examples of the response to TSC stimulation before and after spinal cord pithing are presented in Fig. 4. In either protocol, even at substantially higher stimulation currents, spinal cord transection occluded any response to TSC stimulation (T_{TOT} during baseline, 2.93 ± 0.08 s, versus during TSC stimulation, 2.88 ± 0.09 s, N = 5 experiments). Because we observed complete occlusion of the response to TSC stimulation in either protocol, data from both protocols were grouped (Fig. 1C). Note that as the perfusion pressure is largely determined by the pump, rather than the sympathetic drive to the vasculature, spinal cord transection or pithing evoked only a modest reduction in perfusion pressure of ~10 mmHg (data not shown) and did not change the baseline respiratory pattern. Thus, we conclude that the TSC afferents that modulate the respiratory pattern have their central synapse within the thoracic spinal cord.

3.3. Rhythmic stimulation of thoracic sympathetic chain afferents entrains the respiratory rhythm

Because stimulation of TSC afferents evoked a modulation of the respiratory pattern, we hypothesized that rhythmic TSC stimulation could entrain the respiratory rhythm. To test this hypothesis, we applied rhythmic burst stimulation of TSC afferents near the intrinsic frequency of each preparation's respiratory rhythm.

Most, but not all, rhythmic TSC stimulation trials synchronized (entrained) the respiratory rhythm. A representative example of TSC-evoked forcing of the respiratory rhythm is shown in Fig. 5. Interestingly, when rhythmic TSC stimulation entrained the rhythm, we observed a forcing of the respiratory rhythm such that bursts of TSC stimulation occurred during the late-expiratory phase. For the group, the median preferred relative phase difference for trials with significant entrainment was −1.67 ± 1.32 rad. This late-expiratory phase locking contrasts with the post-inspiratory phase locking evoked by rhythmic activation of the Hering-Breuer reflex circuit (Dhingra et al., 2017, 2013; Dutschmann et al., 2009). Like the forcing evoked by rhythmic activation of the Hering-Breuer reflex, the entrainment evoked by rhythmic TSC stimulation was characterized by periods of stable phase locking interrupted by phase slips (Fig. 5, bottom panel). Flat regions in the plot of the instantaneous relative phase suggest the presence of stable synchronization (arrowheads in Fig. 5). Phase slips (arrows in Fig. 5) are events where the relative phase difference skips a cycle and

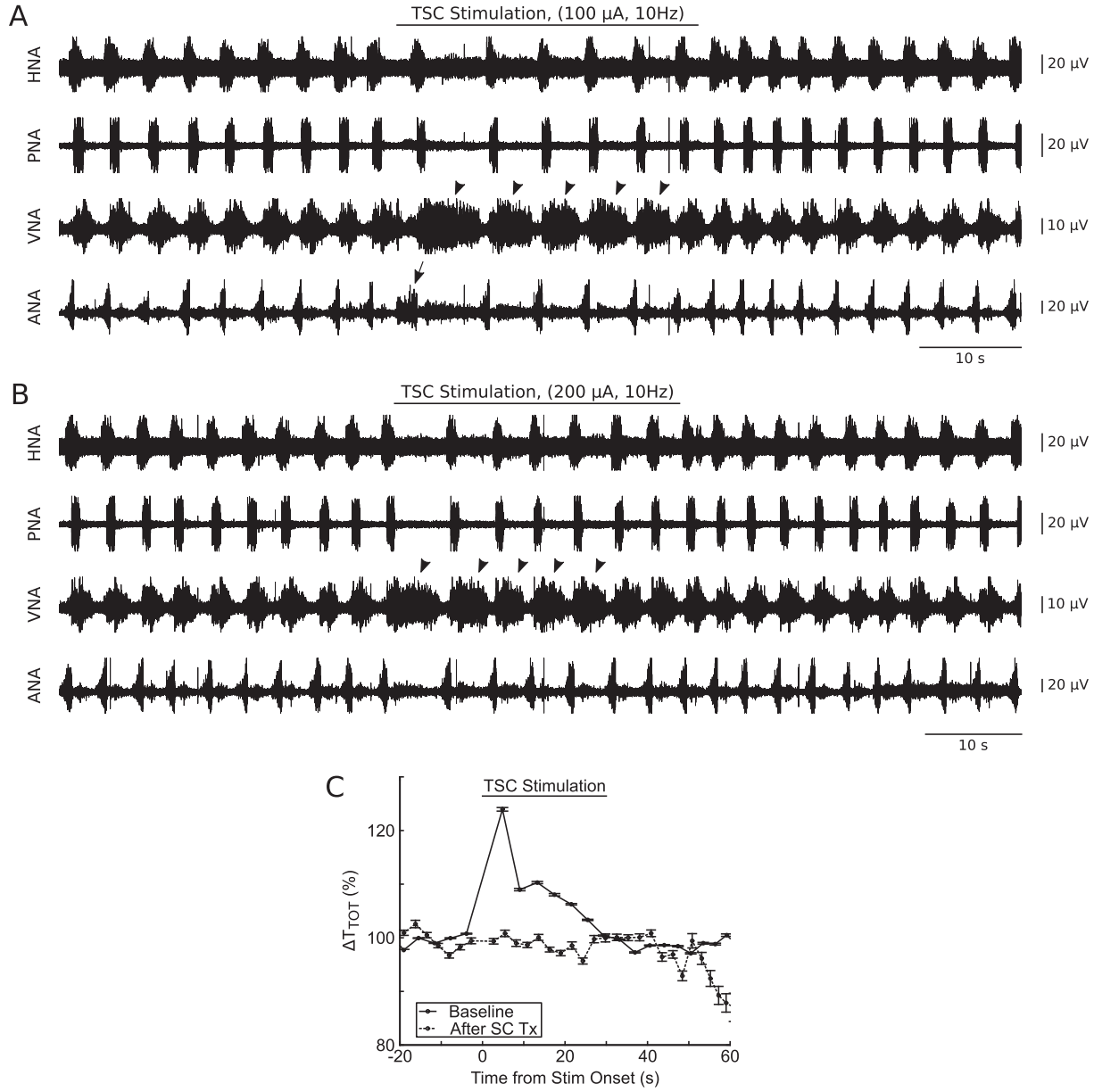

Fig. 1. Stimulation of TSC afferents evoked a slowing of the respiratory rhythm. TSC stimulation typically enhanced post-inspiratory VNA (A & B, arrowheads), but could also enhance ANA (A, arrow) when the stimulus onset occurred near the post-inspiration to late-expiration transition. The response to TSC stimulation rapidly habituated such that the respiratory period returned to near-baseline levels during sustained stimulation. After the stimulus, the respiratory period decreased below baseline levels. The post-stimulus rebound appeared to involve a modulation of the post-inspiratory, but not late-expiratory phase of the respiratory cycle. The time course of the TSC-evoked modulation of the respiratory rhythm is shown before and after spinal cord transection or pithing (C). After spinal cord transection or pithing, we no longer observed any significant TSC-evoked changes in the respiratory rhythm (N = 13 Control; N = 5 SC Tx). Note that data are presented as mean ± SEM.

HNA: hypoglossal nerve activity; PNA: phrenic nerve activity; VNA: vagal nerve activity; ANA: abdominal/illiohypogastric nerve activity; SC Tx: spinal cord transection.

gradually returns to the stably synchronized state. A representative example wherein rhythmic TSC stimulation did not evoke entrainment of the respiratory rhythm is shown in Fig. 6. In such cases, we observed a constant drift between the instantaneous phase of the TSC stimulus and that of the respiratory rhythm (Fig. 6, bottom panel). Note that in this representative trial, we observed strong late-expiratory activity on the ANA before and during rhythmic TSC stimulation suggesting that the thoracic and lumbar spinal cord were well perfused.

To determine the statistical significance and strength of synchronization evoked by TSC forcing, we measured the mutual information between the instantaneous phases of the respiratory rhythm derived from PNA and that of the TSC stimulus. The significance of the entrainment interaction observed in each trial was determined by shuffling the instantaneous phases of either time series and measuring the mutual information for all surrogate time series. The distribution of the mutual information of the original and surrogate datasets is shown in Fig. 7. In ~70% of all TSC entrainment trials (n = 20/28 trials), we measured a significant entrainment interaction which was indicated when the original mutual information of the instantaneous phases (Fig. 7, stars) was greater than that of the 99% confidence interval of the surrogate distribution (Fig. 7, gray bars).

To ensure that the failure of rhythmic TSC stimulation to entrain the respiratory rhythm in some trials was not simply due to a sub-optimal selection of stimulus parameters, we examined the relationship of the

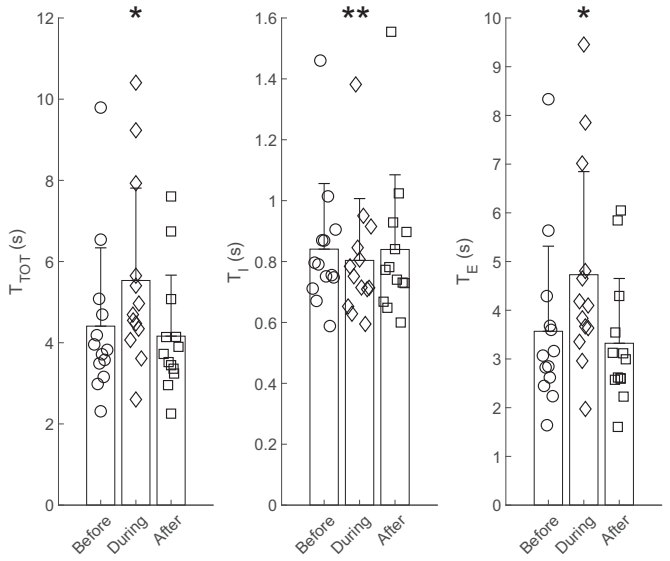

Fig. 2. TSC stimulation increases expiratory phase durations and decreases inspiratory phase durations. For the group, we observed a significant increase of the respiratory period (T_{TOT}) due to significant changes in both inspiratory (T_I) and expiratory (T_E) phase durations. * $p < 0.05$, ** $p < 0.01$.

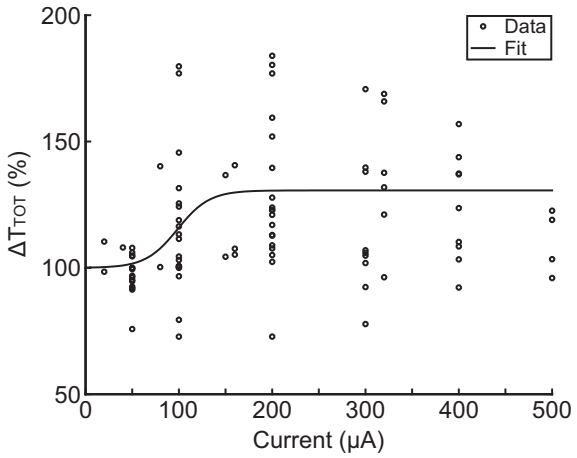

Fig. 3. TSC stimulation evoked an all-or-nothing response. The threshold current necessary to modulate the respiratory pattern was 98.7 μA. The mean maximal change in the respiratory period was 30.6%. $R^2 = 0.117$, $p = 2.7 \times 10^{-8}$.

frequency difference between the intrinsic frequency of the respiratory rhythm and that of the stimulus versus the strength of the observed synchronization interaction (Fig. 8). Because the mutual information of the instantaneous phases quantifies the strength of the phase locking interaction, one should expect that this plot will resemble the Arnold tongues that delineate the stable 1:1 phase locking region between TSC inputs and the respiratory rhythm. Surprisingly, all trials were highly clustered such that trials in which rhythmic TSC stimulation did not evoke entrainment of the respiratory rhythm overlapped with those that did evoke significant stable phase locking. Thus, failures of rhythmic TSC stimulation to entrain the respiratory rhythm were truly physiologic, and not due to an artifact in the rhythmic TSC stimulus parameters. Taken together, we conclude that rhythmic activation of the TSC afferents is sufficient to entrain the respiratory rhythm via the late-expiratory phase.

4. Discussion

We have shown that stimulation of the TSC in juvenile rats in situ can evoke a slowing of the respiratory rhythm via TSC afferent projections into the thoracic spinal cord. Further, we demonstrated that rhythmic TSC stimulation is sufficient to entrain the respiratory rhythm. Interestingly, forcing of the respiratory rhythm via the TSC afferent pathway occurred with a preferred phase such that TSC inputs arrived at the onset of the late-expiratory phase.

4.1. TSC-evoked respiratory modulation during tonic stimulation

In the present study, we observed that the respiratory network rapidly habituated to tonic stimulation of TSC afferents despite suprathreshold stimulus current amplitudes (Fig. 1). Similarly, in dogs and monkeys, Kostreva and colleagues also observed an initially strong apnea which decayed back to a resting-like breathing pattern (Kostreva et al., 1978). In humans, Kruta and colleagues also observed a similar adaptation to splanchnic nerve stimulation.

TSC-evoked sensory modulation of respiratory activity shows some overlap with the classic vagally mediated Hering-Breuer-Reflex (HBR) of the pulmonary stretch receptors (Clark and von Euler, 1972; Cohen et al., 1993; Kubin et al., 2006; Zuperku et al., 1982). Previous studies used vagal nerve stimulation to study central mechanisms of the HBR in various animal models (Hayashi et al., 1996; Siniaia et al., 2000; Zuperku et al., 1982), including in the in situ perfused brainstem preparation (Dhingra et al., 2017; Dutschmann et al., 2009). Tonic suprathreshold stimulation of the vagus nerve in situ initially causes an apnea that lasts even longer than the stimulus (Dutschmann et al., 2014). In this study, the authors observed habituation to vagal nerve stimulation after several trials of stimulation. In other studies, habituation within the HBR pathway has been observed within a single sustained tonic stimulation trial (Siniaia et al., 2000). Even this lower bound on the time to habituation of the HBR (~1 min) exceeded the habituation we observed in response to TSC afferent stimulation (30 s) in this study. Thus, the TSC pathway appears to be prone to rapid central habituation. The habituation also suggests that stimulation of TSC afferents with the stimulus parameters used herein may not relate to visceral nociception as previously suggested (see Section 4.3).

An advantage of the perfused preparation is the ease of recording of multiple respiratory motor outputs, especially the abdominal/iliohypogastric nerve (Abdala et al., 2008; Jones et al., 2016; Magalhães et al., 2018). Previous investigation of the effect of TSC afferent stimulation on respiration used airflow, chest movement, or diaphragmatic electromyographic recordings to assess the functional impact of TSC stimulation (Kostreva et al., 1978; Kruta et al., 1950). Consequently, in the present study, we were able to detect a previously unobserved late-expiratory phase dependence of TSC stimulation: sustained stimulation could modulate abdominal respiratory motor output if the stimulus onset occurred near the post-inspiratory to late-expiratory transition. Such an activation of abdominal late-expiratory activity is never observed during the HBR-evoked slowing of respiration.

4.2. TSC-evoked entrainment of respiration

In the present study, we observed that rhythmic TSC was sufficient to evoke a significant forcing of the respiratory rhythm in 70% of all trials. This partial failure to entrain the respiratory rhythm was not simply due to a sub-optimal selection of stimulus parameters because the current amplitude was suprathreshold, and the frequency difference between the rhythmic TSC stimulus was matched to that of each individual preparation. In previous work, following an identical protocol, we have shown that rhythmic vagal nerve stimulation is sufficient to entrain the respiratory rhythm in 98% of all trials (Dhingra et al., 2017). Together, these observations support the conclusion that lower

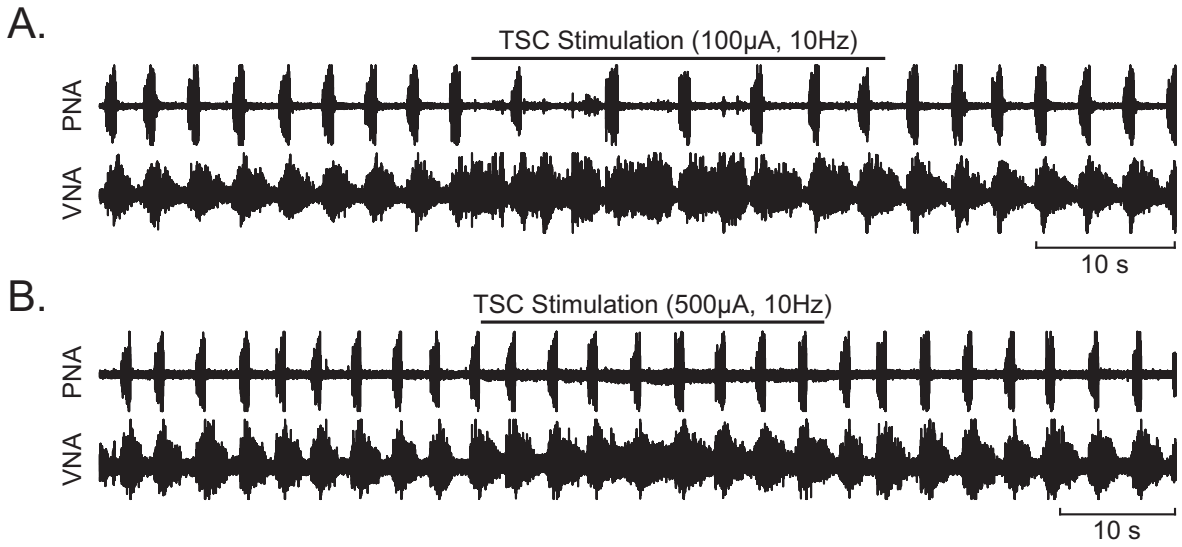

Fig. 4. TSC afferents modulate the respiratory pattern via projections into the thoracic spinal cord. Representative examples of the response to TSC stimulation are shown before (A) and after (B) pithing of the thoracic spinal cord. In all experiments, transection or pithing of the thoracic spinal cord abolished the response to TSC stimulation. Note that the traces are plotted on different time scales.

TSC afferents have a weaker influence on the respiratory rhythm than vagal HBR afferents.

More strikingly, rhythmic TSC stimulation evoked phase locking of the respiratory rhythm in the late-expiratory phase. In contrast, rhythmic activation of the HBR via rhythmic vagal stimulation or lung inflation in the perfused brainstem entrained the respiratory rhythm on the inspiratory off-switch (Dhingra et al., 2017; Dutschmann et al., 2009). Because higher thoracic sympathetic afferents have been shown to have respiratory modulated activity on a breath-by-breath basis (Kostreva et al., 1975), the observation of a late-expiratory preferred phase suggests that TSC afferents from lower thoracic segments may be typically active during the late-expiratory phase when abdominal musculature is activated. In support of this hypothesis, recordings of intra-abdominal pressure during quiet breathing in humans have demonstrated a breath-by-breath modulation (Bishop, 1963; Campbell and Green, 1953). Alternatively, TSC afferent pathways may be subject

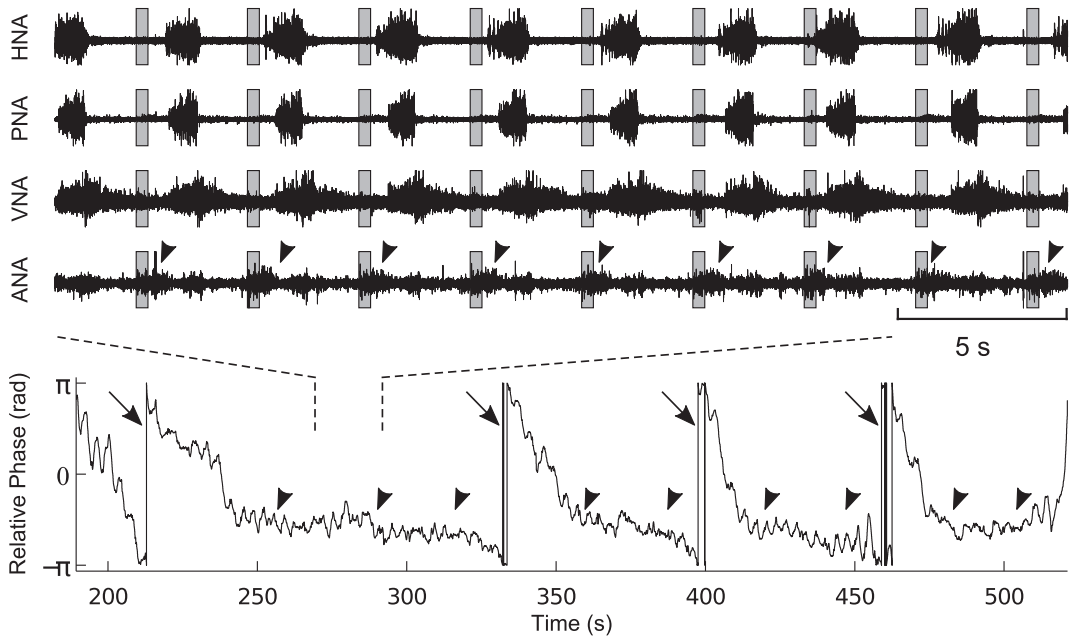

Fig. 5. The respiratory network can be entrained by rhythmic TSC stimulation. Representative traces (top panel) of the fictive respiratory rhythm and the rhythmic TSC stimulus (top panel, gray bars) and the instantaneous relative phase (bottom panel) are shown in a case where rhythmic TSC stimulation entrained the respiratory rhythm. Dashed lines in the instantaneous relative phase plot (bottom panel) indicate the epoch that corresponds to the representative traces (top panel). Flat regions in the plot of the instantaneous relative phase indicate the presence of stable synchronization. Like entrainment via the vagal HBR pathway, TSC entrainment was characterized by epochs of stable synchronization (arrowheads in bottom panel, e.g., periods with a constant relative phase) interrupted by phase slips (arrows in bottom panel). The preferred relative phase for this epoch was -1.83 ± 1.14 rad, which corresponds to a relative phase where the TSC stimulus impinges on the respiratory network near the onset of late-expiration. This timing of the entrainment interaction was also visible in the raw traces since the stimulus arrived precisely at the onset of ANA during synchronized epochs. Finally, the raw traces also suggest that rhythmic TSC stimulation can evoke ANA (i.e., arrowheads in top panel identify additional ANA bursts that occur immediately after the TSC stimulus).

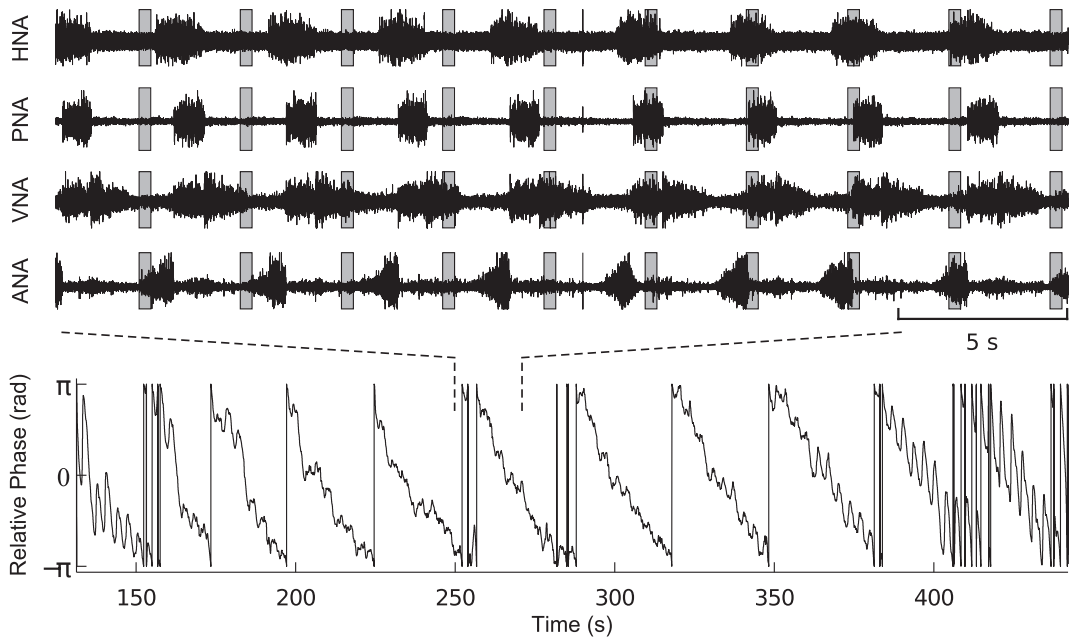

Fig. 6. Representative example of rhythmic TSC stimulation that does not entrain the respiratory rhythm. Representative traces (top panel) of the fictive respiratory rhythm and the rhythmic TSC stimulus (gray bars) and the instantaneous relative phase (bottom panel) are shown in a case where rhythmic TSC stimulation did not evoke significant entrainment. Dashed lines in the instantaneous relative phase plot (bottom panel) indicate the epoch that corresponds to the representative traces (top panel). In this example, the relative phase between the TSC stimulus and PNA continually drifted. This failure of rhythmic TSC stimulation to entrain the respiratory rhythm was not due to under-perfusion of the thoracic spinal cord since we also observed robust late-expiratory activity in ANA.

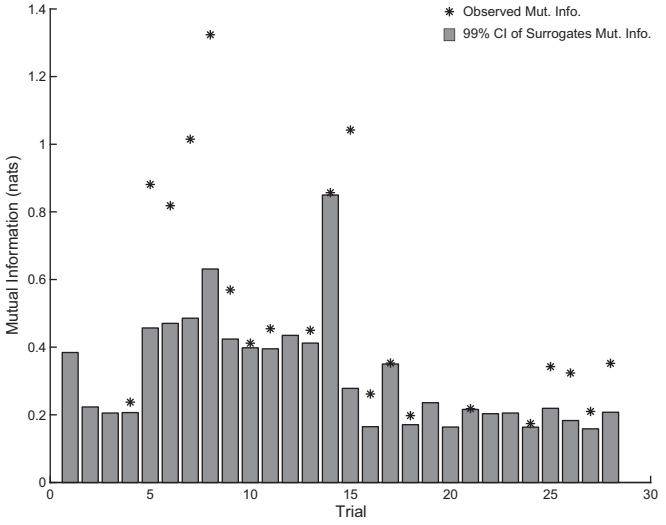

Fig. 7. The strength of TSC-evoked entrainment is consistent with weak forcing. To determine the statistical significance of the TSC-evoked entrainment of the respiratory rhythm, we compared the mutual information of the original instantaneous phase timeseries' with the mutual information of a surrogate data set that was generated by shuffling whole cycles of the instantaneous phases of the original time series. In this plot, gray bars indicate the upper bound of the 99% confidence interval of the surrogate dataset. Trials were considered to show a significant interaction if the mutual information of the original time series was greater than that of the surrogates (where significant, black stars plot the observed mutual information of the instantaneous phases). We observed a significant entrainment of the respiratory rhythm in 70% of rhythmic TSC stimulation trials.

to a gating of these inputs onto the ponto-medullary respiratory network that differs from the gating that influences HBR inputs (Eldridge and Millhorn, 1986).

4.3. The physiological role of TSC-evoked respiratory modulation

Visceral spinal afferents coursing through sympathetic nerves have been studied largely in the context of visceral nociception (for review, see Cervero, 1994; Cervero and Jänig, 1992; Jänig, 1996). It was shown that upper thoracic TSC afferents have discharge patterns that were tightly coupled to lung volume (Kostreva et al., 1975) suggesting that pulmonary afferents may travel through sympathetic nerves. Note that in the perfused preparation, we cannot determine the origin of the stimulated visceral afferents because they are removed during dissection. However, because we stimulated the sympathetic chain between T7 and T10, it is likely that these afferents arose in the abdominal viscera. Moreover, as discussed above, our experiments showed that TSC afferents synchronize the respiratory pattern via the transition from post-inspiration to late-expiration (e.g. mid-expiration). In contrast, pulmonary reflexes typically target late-inspiration or post-inspiration. Thus, we suggest that TSC afferents may convey respiratory-related sensory feedback not from the lungs, but instead from abdominal viscera. Indeed, intra-abdominal pressure during quiet breathing in humans is modulated by respiration (Bishop, 1963; Campbell and Green, 1953). Thus, we speculate that sensory feedback conveyed by TSC afferents might relate to visceral mass movement (within the trunk) that are thought to contribute to locomotor–respiratory coupling during exercise (e.g. walking trotting, galloping or running) in a variety of mammalian species (Alexander, 1993; Bramble and Carrier, 1983; Simons, 1999). In humans, diaphragm function and airflow patterns are also reported to be influenced by the transient axial acceleration of abdominal viscera (Brown et al., 2004; Loring et al., 2001; Wilson and Liu, 1994). A role of TSC afferents in locomotor–respiratory coupling is further supported by a previous study that showed that stable entrainment of respiration by somatic sensory stimulation, as a model for locomotor–respiratory coupling in the perfused brainstem preparation, occurred only when stimuli were delivered during mid-/late-expiration (Potts et al., 2005). Taken together, we conclude that TSC afferents may provide sensory feedback related to the movement of the viscera that in turn contributes to the modulation of respiration, particularly during

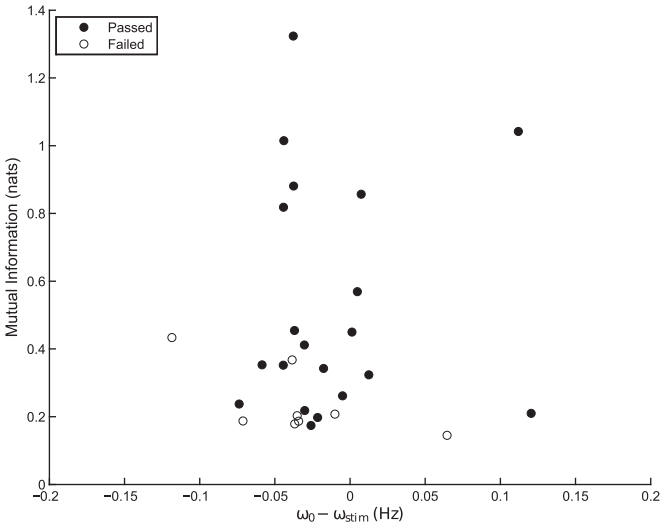

Fig. 8. Rhythmic TSC stimulation parameters do not predict the absence of significant respiratory rhythm entrainment. One possibility to account for the failure of rhythmic TSC stimulation to entrain the respiratory rhythm in some trials (open circles) is that the frequency difference between the respiratory rhythm and the rhythmic TSC stimulus ($\omega_0 - \omega_{stim}$) were not selected to evoke maximal synchronization. However, we observed no correlation between this frequency difference and the observed mutual information of the instantaneous phases. Moreover, the TSC current amplitudes used were always at least 1.5× the threshold current necessary to evoke HBR-like modulation of the respiratory pattern. Thus, we conclude that these trials reflected a physiologic gating of the TSC afferent input.

locomotor–respiratory coupling.

Acknowledgements

This work was supported by the National Institutes of Health [NIH 1OT1TR001779-01] and the Australian Research Council [DP170104861].

References

Abdala, A.P.L., Rybak, I.A., Smith, J.C., Paton, J.F.R., 2008. Abdominal expiratory activity in the rat brainstem–spinal cord in situ: patterns, origins and implications for respiratory rhythm generation. J. Physiol. 587, 3539–3559. https://doi.org/10.1113/jphysiol.2008.167502.

Alexander, R.M., 1993. Breathing while trotting. Science 262, 196–197. https://doi.org/10.1126/science.8211137.

Ausborn, J., Koizumi, H., Barnett, W.H., John, T.T., Zhang, R., Molkov, Y.I., Smith, J.C., Rybak, I.A., 2018. Organization of the core respiratory network: insights from optogenetic and modeling studies. PLoS Comput. Biol. 14, e1006148. https://doi.org/10.1371/journal.pcbi.1006148.

Bautista, T.G., Dutschmann, M., 2014. Ponto-medullary nuclei involved in the generation of sequential pharyngeal swallowing and concomitant protective laryngeal adduction in situ. J. Physiol. 592, 2605–2623. https://doi.org/10.1113/jphysiol.2014.272468.

Biscoe, T.J., Taylor, A., 1963. The discharge pattern recorded in chemoreceptor afferent fibres from the cat carotid body with normal circulation and during perfusion. J. Physiol. 168, 332–344. https://doi.org/10.1113/jphysiol.1963.sp007195.

Bishop, B., 1963. Abdominal muscle and diaphragm activities and cavity pressures in pressure breathing. J. Appl. Physiol. 18, 37–42. https://doi.org/10.1152/jappl.1963.18.1.37.

Bolser, D.C., Pitts, T.E., Davenport, P.W., Morris, K.F., 2015. Role of the dorsal medulla in the neurogenesis of airway protection. Pulm. Pharmacol. Ther. 35, 105–110. https://doi.org/10.1016/j.pupt.2015.10.012.

Bramble, D.M., Carrier, D.R., 1983. Running and breathing in mammals. Science 219, 251–256. https://doi.org/10.1126/science.6849136.

Brown, R.E., Lee, H., Loring, S.H., 2004. Airflow synchronous with oscillatory acceleration reflects involuntary respiratory muscle activity. Respir. Physiol. Neurobiol. 140, 265–282. https://doi.org/10.1016/j.resp.2004.02.007.

Campbell, E.J.M., Green, J.H., 1953. The variations in intra-abdominal pressure and the activity of the abdominal muscles during breathing; a study in man. J. Physiol. 122, 282–290. https://doi.org/10.1113/jphysiol.1953.sp004999.

Cervero, F., 1985. Visceral nociception: peripheral and central aspects of visceral nociceptive systems. Philos. Trans. R. Soc. Lond. Ser. B Biol. Sci. 308, 325–337.

Cervero, F., 1994. Sensory innervation of the viscera: peripheral basis of visceral pain. Physiol. Rev. 74, 95–138. https://doi.org/10.1152/physrev.1994.74.1.95.

Cervero, F., Jänig, W., 1992. Visceral nociceptors: a new world order? Trends Neurosci. 15, 374–378. https://doi.org/10.1016/0166-2236(92)90182-8.

Clark, F.J., von Euler, C., 1972. On the regulation of depth and rate of breathing. J. Physiol. 222, 267–295. https://doi.org/10.1113/jphysiol.1972.sp009797.

Cohen, M.I., Huang, W.X., Barnhardt, R., See, W.R., 1993. Timing of medullary late-inspiratory neuron discharges: vagal afferent effects indicate possible off-switch function. J. Neurophysiol. 69, 1784–1787. https://doi.org/10.1152/jn.1993.69.5.1784.

Del Negro, C.A., Funk, G.D., Feldman, J.L., 2018. Breathing matters. Nat. Rev. Neurosci. 1. https://doi.org/10.1038/s41583-018-0003-6.

Dhingra, R.R., Zhu, Y., Jacono, F.J., Katz, D.M., Galan, R.F., Dick, T.E., 2013. Decreased Hering–Breuer input-output entrainment in a mouse model of Rett syndrome. Front. Neural Circuits 7. https://doi.org/10.3389/fncir.2013.00042.

Dhingra, R.R., Dutschmann, M., Galán, R.F., Dick, T.E., 2017. Kölliker-Fuse nuclei regulate respiratory rhythm variability via a gain-control mechanism. Am. J. Phys. Regul. Integr. Comp. Phys. 312, R172–R188. https://doi.org/10.1152/ajpregu.00238.2016.

Dutschmann, M., Dick, T.E., 2012. Pontine mechanisms of respiratory control. Compr. Physiol. 2, 2443–2469. https://doi.org/10.1002/cphy.c100015.

Dutschmann, M., Wilson, R.J.A., Paton, J.F.R., 2000. Respiratory activity in neonatal rats. Auton. Neurosci. 84, 19–29. https://doi.org/10.1016/S1566-0702(00)00177-6.

Dutschmann, M., Mörschel, M., Rybak, I.A., Dick, T.E., 2009. Learning to breathe: control of the inspiratory–expiratory phase transition shifts from sensory- to central-dominated during postnatal development in rats. J. Physiol. 587, 4931–4948. https://doi.org/10.1113/jphysiol.2009.174599.

Dutschmann, M., Bautista, T.G., Mörschel, M., Dick, T.E., 2014. Learning to breathe: habituation of Hering–Breuer inflation reflex emerges with postnatal brainstem maturation. Respir. Physiol. Neurobiol. 195, 44–49. https://doi.org/10.1016/j.resp.2014.02.009.

Eldridge, F.L., Millhorn, D.E., 1986. Oscillation, gating, and memory in the respiratory control system. In: Comprehensive Physiology. Wiley-Blackwell, pp. 93–114. https://doi.org/10.1002/cphy.cp030203.

Eyzaguirre, C., Lewin, J., 1961. The effect of sympathetic stimulation on carotid nerve activity. J. Physiol. 159, 251.

Hayashi, F., Coles, S.K., McCrimmon, D.R., 1996. Respiratory neurons mediating the Breuer–Hering reflex prolongation of expiration in rat. J. Neurosci. 16, 6526–6536. https://doi.org/10.1523/JNEUROSCI.16-20-06526.1996.

Jänig, W., 1996. Neurobiology of visceral afferent neurons: neuroanatomy, functions, organ regulations and sensations. Biol. Psychol. 42, 29–51. https://doi.org/10.1016/0301-0511(95)05145-7.

Jean, A., 2001. Brain stem control of swallowing: neuronal network and cellular mechanisms. Physiol. Rev. 81, 929–969. https://doi.org/10.1152/physrev.2001.81.2.929.

Jones, S.E., Stanić, D., Dutschmann, M., 2016. Dorsal and ventral aspects of the most caudal medullary reticular formation have differential roles in modulation and formation of the respiratory motor pattern in rat. Brain Struct. Funct. 221, 4353–4368. https://doi.org/10.1007/s00429-015-1165-x.

Kostreva, D.R., Zuperku, E.J., Hess, G.L., Coon, R.L., Kampine, J.P., 1975. Pulmonary afferent activity recorded from sympathetic nerves. J. Appl. Physiol. 39, 37–40.

Kostreva, D.R., Hopp, F.A., Zuperku, E.J., Igler, F.O., Coon, R.L., Kampine, J.P., 1978. Respiratory inhibition with sympathetic afferent stimulation in the canine and primate. J. Appl. Physiol. 44, 718–724.

Kralemann, B., Cimponeriu, L., Rosenblum, M., Pikovsky, A., Mrowka, R., 2008. Phase dynamics of coupled oscillators reconstructed from data. Phys. Rev. E 77. https://doi.org/10.1103/PhysRevE.77.066205.

Kruta, V., Bedrna, J., Prochazka, J., Volf, J., 1950. Influence de la Stimulation Afférente du Nerf Splanchnique sur Les Mouvements Respiratoires chez L'Homme. Arch. Int. Physiol. 58, 90–100. https://doi.org/10.3109/13813455009144941.

Kubin, L., Alheid, G.F., Zuperku, E.J., McCrimmon, D.R., 2006. Central pathways of pulmonary and lower airway vagal afferents. J. Appl. Physiol. 101, 618–627. https://doi.org/10.1152/japplphysiol.00252.2006.

Lindsey, B.G., Rybak, I.A., Smith, J.C., 2012. Computational models and emergent properties of respiratory neural networks. Compr. Physiol. 2, 1619–1670. https://doi.org/10.1002/cphy.c110016.

Loring, S.H., Lee, H.-T., Butler, J.P., 2001. Respiratory effects of transient axial acceleration. J. Appl. Physiol. 90, 2141–2150. https://doi.org/10.1152/jappl.2001.90.6.2141.

Magalhães, K.S., Spiller, P.F., da Silva, M.P., Kuntze, L.B., Paton, J.F.R., Machado, B.H., Moraes, D.J.A., 2018. Locus Coeruleus as a vigilance centre for active inspiration and expiration in rats. Sci. Rep. 8 (15654). https://doi.org/10.1038/s41598-018-34047-w.

Mutolo, D., 2017. Brainstem mechanisms underlying the cough reflex and its regulation. Respir. Physiol. Neurobiol. 243, 60–76. https://doi.org/10.1016/j.resp.2017.05.008.

Oku, Y., Dick, T.E., 1992. Phase resetting of the respiratory cycle before and after unilateral pontine lesion in cat. J. Appl. Physiol. 72, 721–730. https://doi.org/10.1152/jappl.1992.72.2.721.

Oku, Y., Dick, T.E., Cherniack, N.S., 1993. Phase-dependent dynamic responses of respiratory motor activities following perturbation of the cycle in the cat. J. Physiol. 461, 321–337. https://doi.org/10.1113/jphysiol.1993.sp019516.

Ossipov, M.H., Dussor, G.O., Porreca, F., 2010. Central modulation of pain. J. Clin. Invest. 120, 3779–3787. https://doi.org/10.1172/JCI43766.

Paton, J.F.R., 1996. A working heart-brainstem preparation of the mouse. J. Neurosci. Methods 65, 63–68. https://doi.org/10.1016/0165-0270(95)00147-6.

Pérez de los Cobos Pallares, F., Bautista, T.G., Stanić, D., Egger, V., Dutschmann, M., 2016. Brainstem-mediated sniffing and respiratory modulation during odor

stimulation. Respir. Physiol. Neurobiol. 233, 17–24. https://doi.org/10.1016/j.resp.2016.07.008.
Potts, J.T., Rybak, I.A., Paton, J.F.R., 2005. Respiratory rhythm entrainment by somatic afferent stimulation. J. Neurosci. 25, 1965–1978. https://doi.org/10.1523/JNEUROSCI.3881-04.2005.
Prabhakar, N.R., Peng, Y.-J., 2004. Peripheral chemoreceptors in health and disease. J. Appl. Physiol. 96, 359–366. https://doi.org/10.1152/japplphysiol.00809.2003.
Ramirez, J.-M., Baertsch, N.A., 2018. The dynamic basis of respiratory rhythm generation: one breath at a time. Annu. Rev. Neurosci. https://doi.org/10.1146/annurev-neuro-080317-061756.
Romaniuk, J.R., Supinski, G.S., DiMarco, A.F., 1993. Reflex control of diaphragm activation by thoracic afferents. J. Appl. Physiol. 75, 63–69. https://doi.org/10.1152/jappl.1993.75.1.63.
Simons, R.S., 1999. Running, breathing and visceral motion in the domestic rabbit (Oryctolagus cuniculus): testing visceral displacement hypotheses. J. Exp. Biol. 202, 563–577.
Siniaia, M.S., Young, D.L., Poon, C.-S., 2000. Habituation and desensitization of the Hering-Breuer reflex in rat. J. Physiol. 523, 479–491. https://doi.org/10.1111/j.1469-7793.2000.t01-1-00479.x.
Smith, J.C., Abdala, A.P.L., Rybak, I.A., Paton, J.F.R., 2009. Structural and functional architecture of respiratory networks in the mammalian brainstem. Philos. Trans.: Biol. Sci. 364, 2577–2587.
Taylor, A., 1968. The Discharge Pattern of Single Carotid Body Chemoreceptor Units in Relation to Possible Sensory Mechanisms. Arter. Chemorecept. Blackwell Oxf., pp. 195–204.
von Euler, C., 1980. Central pattern generation during breathing. Trends Neurosci. 3, 275–277. https://doi.org/10.1016/0166-2236(80)90100-9.
Wilson, T.A., Liu, S., 1994. Effect of acceleration on the chest wall. J. Appl. Physiol. 76, 1242–1246. https://doi.org/10.1152/jappl.1994.76.3.1242.
Zhu, Y., Hsieh, Y.-H., Dhingra, R.R., Dick, T.E., Jacono, F.J., Galán, R.F., 2013. Quantifying interactions between real oscillators with information theory and phase models: application to cardiorespiratory coupling. Phys. Rev. E 87. https://doi.org/10.1103/PhysRevE.87.022709.
Zuperku, E.J., Hopp, F.A., Kampine, J.P., 1982. Central integration of pulmonary stretch receptor input in the control of expiration. J. Appl. Physiol. 52, 1296–1315. https://doi.org/10.1152/jappl.1982.52.5.1296.